Disulfide Trapping the Mechanosensitive Channel MscL into a Gating-Transition State

Irene Iscla, Gal Levin, Robin Wray, and Paul Blount
Department of Physiology, University of Texas-Southwestern Medical Center, Dallas, Texas

ABSTRACT The mechanosensitive channel of large conductance, MscL, serves as a biological emergency release valve protecting bacteria from acute osmotic downshock, and is to date the best characterized mechanosensitive channel. The N-terminal region of the protein has been shown to be critical for function by random, site-directed, and deletion mutagenesis, yet is structurally poorly understood. One model proposes that the extreme N-termini form a cluster of amphipathic helices that serves as a cytoplasmic second gate, separated from the pore-forming transmembrane domain by a "linker". Here, we have utilized cysteine trapping of single-cysteine mutated channels to determine the proximity, within the homopentameric complex, of residues within and just peripheral to this proposed linker. Our results indicate that all residues in this region can form disulfide bridges, and that the percentage of dimers increases when the channel is gated in vivo. Functional studies suggest that oxidation traps one of these mutated channels, N15C, into a gating-transition state that retains the capacity to obtain both fully open and closed states. The data are not easily explained by current models for the smooth transition from closed-to-open states, but predict that an asymmetric movement of one or more of the subunits commonly occurs upon gating.

INTRODUCTION

The ability to detect mechanical stimuli underlies multiple and diverse physiological processes including hearing and touch senses, vestibular function, blood pressure regulation, heart mechanoelectric feedback, gravitropism, and osmoregulation (1–5). Mechanosensitive channels are postulated to be the primary transducers of mechanosensation. But, despite their unquestionable importance, little is known of these channels at the molecular level in higher organisms, primarily because of the complexity of mechanosensory organs and the very low abundance of cells and channels in the systems in which they are found. In contrast, microbial mechanosensitive channels have been extremely tractable, serving as a paradigm for how ion channels can sense and respond to mechanical forces. Four MS channel activities have been characterized in bacteria: the mechanosensitive channel of large conductance, MscL; smaller conductance, MscS; miniconductance, MscM; and one that is K^+-regulated, MscK (6–8). The physiological role of MscS and MscL channels is to act as turgor-operated emergency valves for solute release and rapid homeostatic adjustment in the event of an osmotic downshock (sudden change to a lower osmolarity environment). Indeed, a Δ*mscL*/Δ*mscS* double mutant bacterial strain shows more than a 10-fold increase in cell lysis upon osmotic downshock when compared to the parental strain (9).

The first gene shown to encode a mechanosensitive channel activity is *mscL* from *Escherichia coli* (10). The encoded MscL protein (Eco-MscL) is relatively small consisting of 136 amino acids with two transmembrane domains (TM1 and TM2), a periplasmic loop, and both the amino and carboxyl terminal facing the cytoplasm (11). Several studies utilizing random and site-directed mutagenesis have identified the most cytoplasmic region of TM1 as essential for normal channel activity, and have lead to the postulation of a gating mechanism (12,13). The crystallization and structural resolution to 3.5 Å of the *Mycobacterium tuberculosis* ortholog (Tb-MscL) in the closed, or nearly closed, state confirmed the previous topological analysis of Eco-MscL (11) and revealed that the channel is a homopentamer (14). Two models have been proposed for the structure of Eco-MscL. First, Sukharev, Guy, and their colleagues (15,16) generated detailed structural models (SG model) of Eco-MscL in its closed, open, and transitional states during gating, based on the Tb-MscL crystal structure, molecular modeling, and disulfide trapping experiments. A second model of MscL gating was proposed by Perozo, Martinac, and their colleagues (PM model), and was based on data from site-directed spin-labeling (SDSL) and electron paramagnetic resonance (EPR) spectroscopy studies (17). Both models propose that a sharp tilting of the transmembrane domains toward the plane of the membrane occurs during gating. Although the two models disagreed on the direction and degree of the rotation of the TM1 helix, thus predicting a completely different set of residues to line the pore in the open state, a resolution to this discrepancy, largely consistent with the PM model, has recently been proposed (18).

Submitted June 1, 2006, and accepted for publication October 20, 2006.

Address reprint requests to Paul Blount, Dept. of Physiology, University of Texas-Southwestern Medical Center, 5323 Harry Hines Blvd., Dallas, TX 75390-9040. Tel.: 214-645-6014; Fax: 214-645-6019; E-mail: paul.blount@utsouthwestern.edu.

Gal Levin's present address is Dept. of Neurobiology, University of Pittsburgh School of Medicine, 6068 BST3, 3501 Fifth Ave., Pittsburgh, PA 15261.

Abbreviations used: MS, mechanosensitive; TM, transmembrane domain; GOF, gain-of-function; LOF, loss-of-function; *E. coli*, *Escherichia coli*; DTT, dithiothreitol; OD, optical density; P_o, open probability.

0006-3495/07/02/1224/09 $2.00

doi: 10.1529/biophysj.106.090316

The crystallization of Tb-MscL was a breakthrough to the understanding of the channel; however, not all of the protein was resolved, with the extreme N-terminal portion of MscL missing from the crystal structure (starts at residue R11). As mentioned by the authors, residues before V15 are disordered in the crystal, presumably because of a high mobility (14). Although no direct structural data are available, the functional relevance of the N-terminal region has been experimentally demonstrated. Deletion of only 11 amino acids at the MscL extreme N-terminal end leads to a nonfunctional channel (19); random mutagenesis experiments showed that expression of MscL channels with an N15D, G14E, or R13C substitution alters channel function and leads to a slowed-growth gain-of-function (GOF) in vivo phenotype (20). Finally, Kumánovics et al. (21) found a motif, NhhD (where h is hydrophobic), found near the cytoplasmic membrane before a transmembrane domain (N15-D18 in Eco-MscL), is extremely conserved among very diverse families of channels including bacterial MscL, voltage-gated, polycystin, *Drosophila* TRP, and human TRP-like channels. The authors hypothesized that this conserved motif is a functional component of sensor modules; consistent with this interpretation, mutation of this region leads to misfunctioning channels in virtually every sensor-channel family in which it is found (21).

Because of its clear functional importance but lack of structural data, the N-terminal region of MscL remains mysterious. The SG model of Eco-MscL predicted that the N-terminal region forms an α-helix (S1) essential for channel gating. It furthermore predicts that in the pentameric channel the S1 domains form a helical bundle that constitutes a ''second gate''. According to the model, the channel remains closed even after the TM1 domains have accomplished significant tilting within the membrane and have expanded to form a large vestibule. The sequential separation of S1 segments are employed to explain the substates observed in patch clamp (15,16). The delayed expansion of S1 in this model predicted that the three ''linker'' residues, Arg-13, Gly-14, and Asn-15, should be very flexible to serve as a ''string'' linking expanding TMs to the still-closed S1 bundle. As support of their hypothesis, the authors note that the length of this region is highly conserved and there is an essentially invariant glycine at position 14 that has more conformational freedom than other residues (16). In the SG transition-state models, the linker and TM1 domains are predicted to move in a symmetrical, smooth, and orderly manner. The PM model is consistent with aspects of the SG model; residues G14–V17 showed the highest mobility of the TM1 region, possibly reflecting its flexibility (17). Despite the models that have been proposed, the specific movements of the linker domain during the gating process have not been tested.

Here, we have utilized an existing cysteine library (22) and a cysteine-trapping approach to determine the proximity of residues R13–D18 in MscL pentameric structure. Because residues 13–18 are predicted by the SG models to not only contain the ''linker'' between S1 and TM1, but also the first few residues at the beginning of the TM1 domain, for simplicity we refer to this area as the S1-TM1 linker region.

By using an osmotic downshock to gate the channels in vivo, we compare the ability of these cysteine-substituted residues to interact with their counterpart in neighboring subunits in the unstressed and osmotically shocked conditions. Our results suggest that residues in this region often approach each other during the closed-to-open transition. In light of the current models for the gating of MscL, these findings cannot be easily explained unless asymmetric movements between the subunits occur in the gating process. The functional consequences of this interaction for one mutant, N15C, were particularly enlightening: the covalent interaction of this residue within the complex appears to occur rapidly and efficiently, and not only still allows the channel to achieve what appears to be a normal and fully open state, demonstrating the flexibility of the region, but also increases the probability of channel gating by 100-fold. Together, the data suggest that we have trapped the channel into a normal transition state that retains the capacity to attain both closed and fully open states.

MATERIALS AND METHODS

Strains and cell growth

E. coli strain PB104 (*ΔmscL*::*Cm*) (11) was used as host for the pB10 expression constructs (11,19,20,23). PB104 was used for the in vivo cysteine-trapping experiments and for electrophysiological analysis in which MscS was used as an internal control. Cultures were routinely grown in Lennox Broth media (LB) (Fisher Scientific, Pittsburgh, PA) plus ampicillin (100 μg/ml) in a shaker-incubator at 37°C and rotated at 250 cycles per minute. Expression was induced by addition of 1 mM isopropyl-β-D-thiogalactopyranoside (IPTG) (Anatrace, Maumee, OH). Culture growth was measured as the optical density (OD) 600 of the cultures at 30-min intervals.

Western blot analysis

Single colonies were grown in LB in a shaker-incubator at 37°C to an early log phase (OD_{600} of 0.2–0.3), and diluted 1:1 in LB media supplemented with 1 M NaCl. At this point IPTG was added to a final concentration of 1 mM to induce MscL protein expression. Cultures were grown to an OD_{600} of 0.3–0.4 and then diluted 20-fold in prewarmed (37°C) distilled water (shock) or in 500 mM NaCl LB media (mock-shock) and returned to the shaker-incubator for 20 min. Cells were pelleted in a microfuge and resuspended in nonreducing Laemmli buffer (62.5 mM Tris pH 6.8 (Fisher Scientific, Pittsburgh, PA), 25% v/v glycerol, 2% w/v sodium dodecyl sulfate (SDS), 0.01% w/v bromophenol blue (Sigma, St. Louis, MO)) in a final volume normalized by the OD_{600} before dilution. At this point 3% β-mercaptoethanol was added to half of each sample; all samples were heated at 70°C for 4 min and centrifuged for 2 min at 14,000× *g* before resolution in a 4–20% gradient Tris-Cl polyacrylamide gel (Bio-Rad, Hercules, CA). Proteins were electrotransferred to Immobilon polyvinylidene fluoride (PVDF) membranes (Millipore, Billerica, MA) at 100 mV for 70 min. Western blot analysis was performed using primary antibodies against the MscL C-terminus as previously described (19) and the Immobilon Detection Reagents kit (Millipore) according to the manufacturer's instructions. X-ray sensitive film (Blue Bio Film, Denville Scientific, Metuchen, NJ) was exposed to the blotted membranes. Quantification was done by measuring the density of the bands using the Scion Image software (National Institutes of Health).

Electrophysiology

E. coli giant spheroplasts were generated and used in patch-clamp experiments as described previously (12). To ensure there is no channel clustering, which could allow interactions between neighboring channels and complicate the interpretations of the results, we kept the expression levels low by decreasing the induction times to <10 min. Thus, expression level was ~5–20 channels per patch. This was done merely as an added precaution, since, in contrast to MscK (7), no evidence of clustering of MscL channels has been observed either by visualization of channels in spheroplasts (24) or when the number of channels per patch has been monitored ((25); this study). Thus, intercomplex disulfide bridges seem unlikely. Excised, inside-out patches were examined at room temperature under symmetrical conditions using a buffer comprised of 200 mM KCl, 90 mM $MgCl_2$, 10 mM $CaCl_2$, and 5 mM HEPES pH 6 (Sigma, St. Louis, MO). When indicated, 30% H_2O_2 (Sigma) or 1 M dithiothreitol (DTT) (Sigma) were added to, or perfused into the bath to a final concentration of 1–5% v/v or 1–10 mM, respectively.

Recordings were performed at −20 mV (positive pipette). Data were acquired at a sampling rate of 20 kHz with a 5-kHz filter using an AxoPatch 200B amplifier in conjunction with Axoscope software (Axon Instruments, Union City, CA). A piezoelectric pressure transducer (World Precision Instruments, Sarasota, FL) was used to monitor the pressure throughout the experiments. The MscL threshold was defined as the pressure at which openings were observed at least every 0.5–2 s. Measurements before and after treatment were compared. To compare channel tension sensitivity between mutated and wild-type channels, the threshold was expressed as a fraction of the threshold for MscS, which was used as an internal control as previously described (12,19,20). Open probability (P_o) analysis and amplitude measurements were performed using Clampfit9 from Pclamp9, whereas Fetchan6 and Pstat6 from Pclamp8 software were used for kinetics analysis (Axon Instruments).

RESULTS

Residues of the S1-TM1 linker region of MscL show activity-dependent interactions

Although the S1-TM1 linker region of MscL is immediately cytoplasmic to the pore of the channel (see the crystal structure; Fig. 1 *A*), highly conserved (Fig. 1 *B*) and critical for channel function (20,21,26), little is known of its structural and functional properties. To test the proximity of the like residues in the pentameric structure in this region (R13–D18) we scanned an existing cysteine library (22) for interactions that occur in vivo before and subsequent to an osmotic downshock, which has been shown to be a normal stimulus for channel gating (27); such a stimulus has been demonstrated to gate the MscL channel in vivo, even in the presence of all other mechanosensitive channels (28). After such an osmotic downshock (OS) or a dilution into a media of the same osmolarity (mock-shock (MS)), cells were harvested and protein interactions analyzed by monitoring the formation of dimers using Western blot. Note that in contrast to other studies where disulfide trapping was used to assess the proximity of residues within the MscL complex (15,29), we lysed cells immediately after harvesting by solubilizing in SDS Laemmli buffer. This approach was chosen over other widely used lysis methods, such French press, to preferentially monitor disulfide bridges that occur in vivo rather than interactions occurring during the cell disruption or subsequent to protein solubilization in nondenaturing detergent.

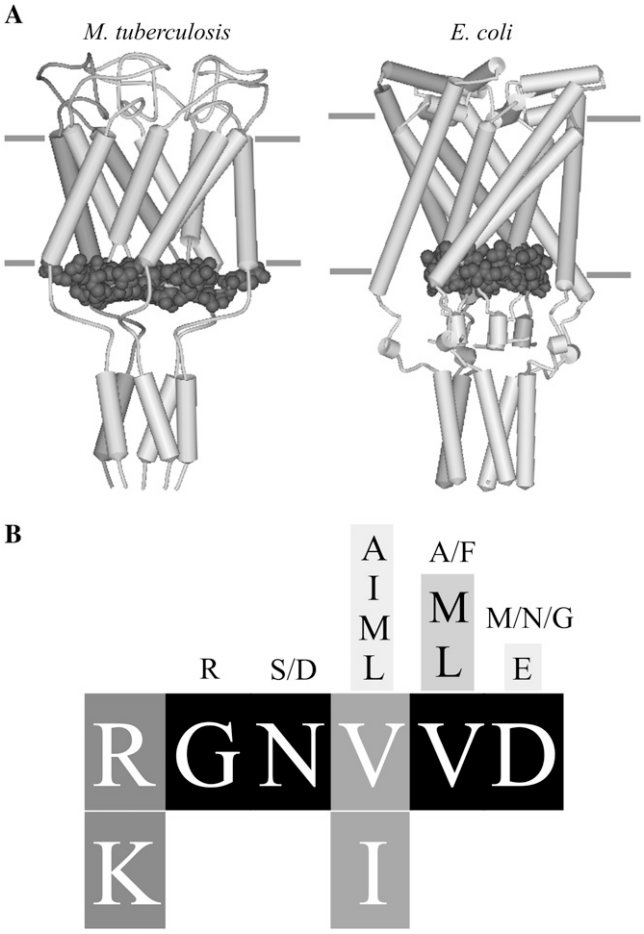

FIGURE 1 Structural localization and conservation of S1-TM1 linker region. (*A*) Schematic representations of MscL based on the *M. tuberculosis* crystal structure (*left*) (14), which some evidence now suggests is in a ''nearly closed'' state (22,33), and the SG model for the closed structure of the *E. coli* MscL that was derived from it (*right*) (15,16). Lateral views of the homopentameric complex are shown with the residues that were cysteine substituted in this study (or the analog in *M. tuberculosis*) highlighted in black (R13–D18 in *E. coli* and R11–D16 in *M. tuberculosis*). (*B*) The result of an alignment of MscL residues R13–D18 from 129 homologs from different species is shown. Larger font sizes and darker boxes reflect more conserved residues. Black boxes are conserved in 80–99% of the aligned species (G14 99%, N15 98%, V16 80%, D18 91%). Dark boxes containing white fonts are conserved in 40–80% (R13 55%, K13 45%). Light gray boxes with white fonts 20–40% (V17 35%, I17 36%); lighter gray boxes with black font 5–20% (M17 14%, L17 11%), while very light gray boxes with letters in black fonts 2–5%, and no box reflects <2%. The alignment was generated using the ClustalW multiple sequence alignment program. A list of the species of the aligned proteins is available in online Supplementary Material.

The results of this scan are shown in Fig. 2. In the absence of an osmotic downshock, only N15C and D18C consistently formed significant amounts of dimers, with less dimerization observed for the G14C mutant (Fig. 2 *A*, *upper panel*). When the same cells were exposed to an osmotic downshock, all the mutants showed a significant increase in disulfide bridging (Fig. 2 *A*, *lower panel*). The graph in Fig. 2 *B* is a quantification of the data derived from multiple experiments ($n \geq 11$)

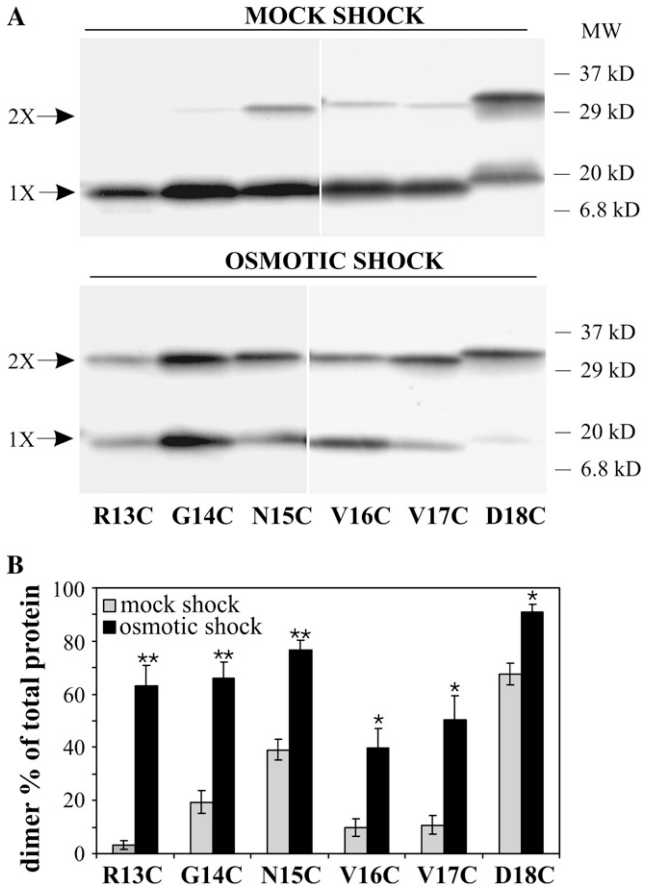

FIGURE 2 Activity-dependent disulfide bridging between residues of the S1-TM1 linker region of MscL. (*A*) Western blots of MscL protein with single-cysteine substitutions; the sites of mutation range from residues R13–D18. Cells expressing each of the mutants were either diluted in a medium of the same osmolarity (mock-shock, *upper panel*) or osmotically downshocked (*lower panel*). MscL protein was found as either a monomer (*1X arrows*) or dimer (*2X arrows*) due to disulfide bridging between cysteines within the pentameric complex. The delayed migration of the monomers and dimers of D18C is consistent, and perhaps due to the removal of the charge. (*B*) Quantification of several experiments similar to the one shown in Fig. 2 *A*. The bars reflect the percentage of MscL protein existing as dimers, calculated from the optical density (represent the mean ± SE from at least 11 independent experiments). Gray bars correspond to mock-shocked whereas black bars correspond to osmotically shocked samples. Student's *t*-test was applied as two-tailed paired for each set (**) $p < 0.00005$, (*) $p < 0.0005$.

similar to the example shown in Fig.2 *A*. The amount of dimers, presented as a percentage of the total MscL, is shown for each mutant after a mock-shock (*gray*) or an osmotic downshock (*black*).

To determine the reversibility and specificity of these reactions, we performed a more detailed set of experiments. As shown in Fig. 3 *A* for the N15C mutant, the observed interactions between MscL subunits could be completely reversed by the presence of the reducing agent β-mercapto-ethanol (βME) as well as DTT, indicating that dimerization was indeed due to disulfide bridge formation by the introduced cysteines. No MscL protein was detected from cells containing only vector, whereas wild-type (WT) MscL showed only monomers and no dimer formation (Fig. 3 *B*). All of the residues in the S1-TM1 linker region showed some dimerization. We therefore sought a negative control to demonstrate that dimerization is not an inherent property of MscL channels that have substitutions in and around this region of the protein. One mutant, I24C, is in a neighboring subdomain and has an α-carbon distance between subunits in the crystal structure (9.34 Å) and the current model of the closed *E. coli* channel (9.97 Å) similar to those in the S1-TM1 linker; however, no dimerization was detected for this mutant, even after the cells were osmotically downshocked (Fig. 3 *B*). Hence, the dimerization observed in the S1-TM1 linker region appears to be specific.

Functional characterization of S1-TM1 linker region mutants

To correlate the structural changes induced by oxidation with the functional changes in channel activity we further characterize the mutants by patch clamp. Unlike the cysteine-trapping experiments described above, oxidizing agents were used in these functional experiments to have a more homogeneous population of channels in the same oxidative state in the patch membrane. Channel activities from giant spheroplasts expressing each of the mutants were studied in reducing and oxidizing conditions (see details in Materials and Methods).

As previously described, R13C activity was rarely observed unless a reducing agent was added to the patch buffer, and under reduced conditions this mutant gates at lower pressures than wild-type MscL (22). In contrast to these data, but consistent with a previous study, the cysteine substitutions at residues G14 and D18 lead to nonfunctional channels that only gated when very high pressures were applied to the patch (21). This observed lack of activity was independent of the presence of a reducing agent in the bath, suggesting that the cysteine substitutions themselves, and not disulfide bridges, produced the observed decrease in functional activity. On the other hand, V16 and V17 cysteine substitutions lead to channel activities with no significant differences from wild-type; no evident changes in their membrane tension sensitivity, conductance, or open probability (P_o) were observed between oxidizing and reducing conditions with full amplitudes achieved in both conditions.

The N15C MscL mutant yielded the most remarkable results of the set in that the biochemical changes were clearly reflected in channel activity, as shown in Fig. 4 *A*. In contrast to mutants showing a decreased activity or lock-closed nature upon oxidation that is observed in other cysteine mutants (above; (15,22)), the P_o of N15C MscL dramatically increased with the addition of 1% H_2O_2 to the patch buffer. Note that a constant pressure was applied to the patch, and that the increase in P_o could be reversed by perfusion with a solution containing 1 mM DTT (Fig. 4 *A*), thus confirming

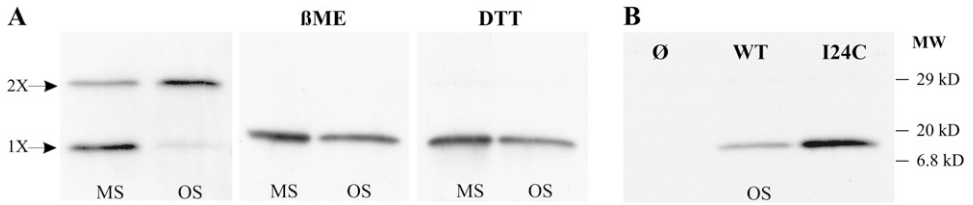

FIGURE 3 Disulfide bridging of MscL is mutant and oxidative-environment dependent. (*A*) Western blot analysis of samples from cells expressing N15C MscL protein after a mock-shock (*MS*) or an osmotic downshock (*OS*). N15C MscL protein exists as a monomer (*1X arrow*) or dimer (*2X arrow*), depending upon whether disulfide bonds are formed (*left panel*). The addition of β-mercapto-ethanol (βME) to a final concentration of 3% or DTT to 100 mM to the N15C samples was sufficient to completely reduce the disulfide bridges between cysteines from different subunits, thus leaving all the protein in its monomeric form (*right panel*). (*B*) Negative controls. Western blot analysis of samples from cells after an osmotic downshock. No MscL protein was detected in cells containing only vector ($\emptyset$), and dimers were absent in cells expressing either wild-type MscL or an independent TM1 MscL cysteine mutant, I24C.

that the observed effects are due to a change in the oxidative state of the channel. Similar results were obtained in multiple experiments and their quantification is shown in Fig. 4 *B*. The histogram of the log of NP_o was plotted versus time and shows that the increase in opening probability occurs within an extremely short timescale, yet is long lasting if kept under nonreduced conditions. Increases in N15C P_o were observed when other oxidative agents such as copper-phenanthroline ($n = 4$) or iodine ($n = 3$) were added to the bath, whereas none of these oxidative agents affected WT MscL activity (see supplemental figure in Supplementary Material). These results suggest that oxidation traps the N15C MscL channel into a conformation, presumably a normal transition state, which requires less energy for gating the channel.

The oxidized form of N15C achieves a normal open state

Although the experiments above demonstrated that under oxidizing conditions the N15C mutant has a higher probability of gating, it does not indicate if a fully open state could be achieved and maintained. To address this question, a more detailed analysis of N15C MscL channel activity was performed, and parameters including threshold, conductance, and kinetics were compared in the presence of 1 mM DTT (reduced conditions) or 1% H_2O_2 (oxidative conditions). Results of these experiments were compared to wild-type MscL values and are summarized in Table 1.

Although the mean threshold for the reduced N15C was slightly higher than that for wild-type, this was not statistically significant. However, as expected from the observed increase in N15C P_o upon oxidation, the pressure required to elicit channel activity in reducing conditions was significantly higher than that required in oxidizing conditions. This is reflected in the threshold values (ratio between MscL threshold and that of the internal control MscS, as described in Materials and Methods) shown in Table 1. Together, those data demonstrate that the observed increase in P_o upon oxidation is due to an increase in sensitivity of the oxidized N15C mutant to membrane tension.

Channel kinetics also correlated with the different oxidative states of the complex. Under reducing conditions (DTT in the patch buffer), N15C activity was characterized by very short open dwell times when compared to those of wild-type

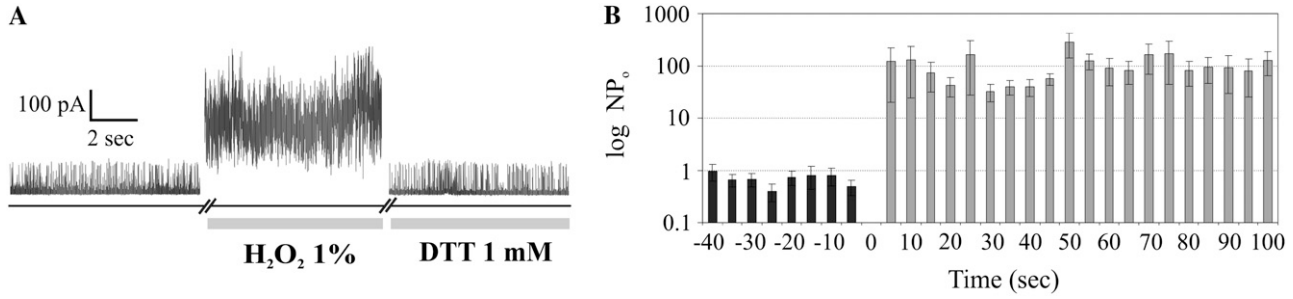

FIGURE 4 The open probability of N15C MscL increases rapidly under oxidative conditions. (*A*) Representative trace of N15C channel activity recorded from an inside-out patch from *E. coli* giant spheroplasts. The reversible effects of oxidation on channel activity are shown. After the addition of H_2O_2, the open probability (P_o) of the channel increased dramatically (~100-fold). This effect could be reversed by perfusion with a solution containing 1 mM of the reducing agent DTT, but absent of the H_2O_2 oxidant. Bars under the trace indicate the time in which the indicated drugs were present in the bath. Although a continuous trace, the double diagonal bars (//) reflect ~15 s of the recording removed during the perfusion. A constant negative pressure of −200 mm Hg was applied to the patch throughout the entire trace shown. (*B*) Quantification of the change in NP_o upon oxidation. NP_o was binned in 5-s time spans with negative values corresponding to the time before the addition of H_2O_2 to the bath. Each recording was normalized independently to the average NP_o values before the treatment. Bars correspond to the mean ± SE of nine experiments. Note that the *y* axis is logarithmic, and that the full effect is seen within the shortest time accurately measured (5 s).

TABLE 1 Electrophysiological characterization of N15C MscL mutant under different oxidative conditions

	Tension sensitivity		Kinetics (ms)	
Strain/Reagent	Threshold MscL/MscS	Amplitude (pA)	τ_2	τ_3
Wild-type	1.55 ± 0.06	81.3 ± 0.9	9.5 ± 3.3	28.3 ± 9.5
N15C/H_2O_2	1.40 ± 0.05*	82.8 ± 0.8	3.8 ± 0.9†	23.8 ± 5.7
N15C/DTT	1.73 ± 0.08§	83.3 ± 0.9	1.0 ± 0.1†‡	5.5 ± 1.1†‡

Tension sensitivity was derived using MscS as an internal control as described in Materials and Methods. Values are the mean ± SE from at least 10 patches that were derived from at least two independent spheroplast preparations. Kinetics were fit assuming three time constants; the shortest (τ 1) is below resolution (<1 ms). Kinetic values were derived from at least 1000 events and two independent spheroplast preparations.

*$p \leq 0.001$, by two-tailed, unpaired Student's t test against wild-type MscL.

$^{\dagger}p \leq 0.0001$, by two-tailed, unpaired Student's t test against wild-type MscL.

$^{\ddagger}p \leq 0.05$, by two-tailed, unpaired Student's t test against H_2O_2 treated.

$^{\S}p \leq 0.001$, by two-tailed, unpaired Student's t test against H_2O_2 treated.

(Fig. 5, *left graph*; Table 1). When experiments were performed in the presence of 1% H_2O_2 (oxidative conditions), longer open dwell times, similar to those of wild-type, were observed (Fig. 5, *right graph*; Table 1). Surprisingly, a full conductance, indistinguishable from wild-type MscL, was observed for N15C not only in reduced but also oxidized conditions (Table 1). In addition, fewer events reached full openings in the reduced state, as can be seen in the inserts in Fig. 5. Hence, even though neighboring subunits are linked by disulfide bridges, as indicated by the biochemical analysis, the channels are actually more likely to obtain a stable and fully conducting open state.

DISCUSSION

Although the S1-TM1 linker region of the MscL protein is extremely conserved (see Fig.1 *B*) and is critical in channel gating (15,16,20,21), its role is not immediately obvious from the crystal structure. Notably, the adjacent N-terminal cytoplasmic region is not even resolved in the Tb-MscL crystal structure, with the structure starting at R11 (analogous to R13 of Eco-MscL). In the subsequently proposed and more speculative SG model for the gating of Eco-MscL, residues R13–N15 have been postulated to be a linker between two critical domains: a predicted amphipathic α-helix at the extreme N-terminal region of the protein, S1, and the first transmembrane domain, TM1 (15,16). Here, in an attempt to better understand the structural and functional properties of this region in the closed and closed-to-open transition states of the channel, we probed the proximity of residues R13–D18 in the MscL pentameric structure. The results clearly indicate that residues in this region can be in quite close proximity, and some appear to approach their analogous residues on neighboring subunits subsequent to osmotic shock.

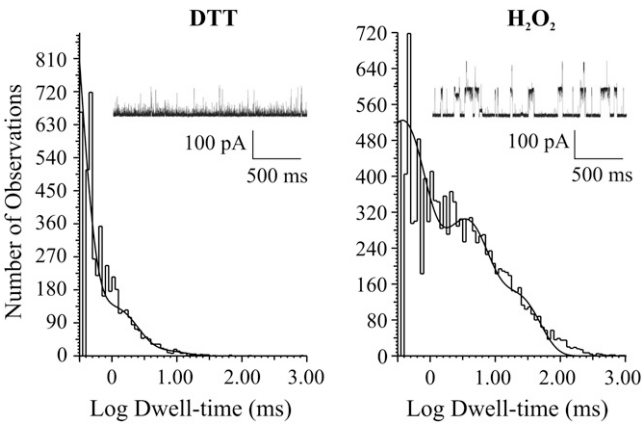

FIGURE 5 Oxidative conditions lead to increased open dwell times of the N15C MscL mutant. The histograms depict the open dwell distribution of N15C in a reduced (*DTT*, *left*) and oxidized (*H_2O_2*, *right*) state. Dwell times were fit with a three components model, as has been described before for wild-type channels and other mutants (19). The inserts within each graph are representative traces of channel activities observed in each condition.

Although the osmotic shock that is used in this study has previously been shown to gate the MscL channel, even when MscS and other channels are expressed (28), one cannot rule out the possibility that an increase in dimerization is due to a more oxidative environment effected by the gating of MS channels. Indeed, the observation that all of the mutants show an increase in dimer formation upon osmotic downshock would be consistent with this interpretation. However, the increase observed is not constant between mutants, as would be expected if redox was the only factor. For example, R13C normally shows a small amount of dimerization that increases >18-fold when subjected to osmotic downshock, whereas V16C and V17C, which also show modest dimerization when untreated, have only a 4–5-fold increase upon osmotic downshock. The most likely interpretation is that the osmotic downshock leads to specific gating transition states, and that each residue has a unique probability for approaching their analogs within the complex and forming dimers upon these structural changes. Hence, whereas changes in the redox environment of the cell play some role in the increase in dimerization observed, it is likely that much of this increase in many of the mutants is due to structural rearrangements that occur as the channel gates.

The finding that the residues within the MscL linker region studied are able to spontaneously disulfide-bridge, or that this ability may increase when MscL is gated, is not predicted by any of the current structural models for the closed, open, or transition states of the channel. To date, the best available

TABLE 2 Predicted distances between α-carbons of residues from neighboring subunits

Tb-MscL residues	Crystal structure	Eco-mscL residues	SG model (closed)	SG model (open)	PM model (open)
R11	18.5	R13	13.0	26.1	N/A
G12	17.6	G14	13.8	25.7	23.7
N13	13.4	N15	10.5	29.0	26.4
I14	9.3	V16	10.6	29.8	25.1
V15	10.5	V17	12.6	30.8	21.0
D16	12.8	D18	10.0	27.9	22.7

The distances between α-carbons of each specified residue from the two closest neighboring subunits. Measurements were made in *M. tuberculosis* using the published crystal structure coordinates (closed state) (14), the in *E. coli* SG model (closed and open states) (15,16), and in *E. coli* PM model (open state) (17) utilizing the ViewerLite program from Accelrys Software (San Diego, CA). All distances are in angstroms.

structural data of MscL are derived from the crystal structure of the Eco-MscL homolog from *M. tuberculosis* (Tb-MscL) that was solved by Chang et al. in its closed or nearly closed state (14) (Fig.1 *A*). The SG model of *E. coli* MscL depicts a detailed gating transition from the closed to the open state of the channel with several intermediate states (15,16). We used these two available closed structures, the Tb-MscL crystal structure and the closed Eco-MscL proposed by SG model (Fig.1 *A*), to determine the predicted distances between the α-carbon atoms from two neighboring subunit residues for R11–D16 in Tb-MscL and the analogous R13–D18 in Eco-MscL. As shown in Table 2, all distances were 9.3 Å or greater, larger than that the 3.6–6.8 Å distance usually required for disulfide bridging two cysteines (30,31). Two models also exist for Eco-MscL in its open state. The SG model, mentioned above, derived from molecular modeling (15,16); a second is the PM model, based on studies using site-directed spin-labeling (SDSL) and electron paramagnetic resonance (EPR) spectroscopy (17,32). In both models, distances between residues in this linker region increase as the channel opens. Measurements of the predicted distances between α-carbons of residues R13–D18 from neighboring subunits in these open-structure models predict an increase in all the distances relative to the closed state (Table 2). Hence, the observed spontaneous bridging between these residues is not easily explained by any current models for the closed or open states.

Although the biochemical data demonstrating the formation of disulfide bridges at several specific locations are irrefutable, some of the electrophysiological studies can be more difficult to interpret due to loss of or unchanging channel activity. For example, consistent with a previous report (22), we find that a cysteine substitution of residue G14 or D18 leads to channels that are not functional in vivo and require very high pressures to open in patch clamp; the presence of a reducing agent did not affect the loss of membrane tension sensitivity of these mutants (this study; (22)). In contrast, V16C and V17C mutants did not show significant differences in in vivo function (22) or in membrane tension sensitivity (this study) when compared to wild-type MscL activity. Here we extend this finding and demonstrate that although disulfide bridges are generated at each of these sites, no significant changes in sensitivity or conductance are observed upon treatment with either H_2O_2 or DTT. This suggests that either the disulfide bridging has no effect, or the bridged channels become less sensitive and are not easily measured. Hence, although the biochemical data demonstrate that activity-modified disulfide bridges occur at these locations, the negative results obtained by patch clamp make the data in these specific instances more difficult to interpret.

Within the S1-TM1 linker region, one residue, R13, has repeatedly been found to be of unique functional importance. In a random mutagenesis study R13C MscL was found to effect a slowed-grow GOF phenotype in vivo (20,22). However, two independent experiments suggest that reconstitution of the charge can remediate the phenotype. First, an in vivo SCAM study demonstrated that an osmotic downshock-induced cell death phenotype of cells expressing this mutant can be partially reversed by the addition of the positively charged MTSET sulfhydryl reagent (18). Second, when R13 was substituted with histidine, the cells expressing the mutated channel showed a GOF phenotype that could be remediated by restoring the positive charge by growth at lower pH (33). Several lines of evidence also suggest that in some conformation(s) the R13 residues are in close proximity. In patch-clamp experiments, the R13H MscL activity was inhibited by the presence of metal ions (33) suggesting a cluster of multiple histidine residues led to metal ion coordination (34–38). In addition, we have demonstrated that in patch clamp, R13C is often found as a locked-closed channel that is best observed in the presence of a reducing agent in the bath (this study; (22)). Finally, here we demonstrate that disulfide bridges at R13 are more likely to be observed in vivo when the channel is gated by osmotic downshock. These results are all consistent with the hypothesis that in the pentameric structure the normally positively charged arginines from each subunit approach each other during the closed-to-open transition; the lack of a charged residue at this position lowers the energy required for the channel to open, thus leading to a GOF phenotype.

Of all residues within the region studied here, N15C gave the most interpretable and surprising results. The findings that dimerization in vivo was increased upon osmotic downshock and, more significantly, that oxidative conditions increase the probability of channel opening in patch clamp strongly suggest that disulfide bridge formation occurs in a closed-to-open transition state. But, does this occur in a normal

transition state or in a state tangential to the normal gating pathway? Put another way, one possible explanation for the data is that the region is extremely flexible, and that at some rate random movements allow the channel to get trapped in a rarely observed state. Indeed, both the SG (16) and PM (17) models predict this region of the channel to be flexible, which is consistent with our observation that the oxidized N15C mutant can obtain fully closed and open states. However, in patch clamp the modification of the channel activity of the N15C mutated channel occurs as rapidly as can be measured after an oxidizing agent is added to the bath (see Fig. 4). Hence, not only does it appear that N15 residues *can* approach their counterparts in neighboring subunits upon gating, it also seems extremely likely that this movement is quite common, probably occurring in the vast number of gating events.

One might expect from disulfide trapping experiments, like those presented here, that such a covalent linkage would lead to channels or proteins ''locked'' into specific conformations. In reality, however, the trapped state may not be immobile. For example, the Tb-MscL V15C mutant (corresponding to V17C in Eco-MscL), under oxidative conditions, has previously been found to lock into an open state in response to pressure; the channel then slowly and irreversibly stabilized into partially open ''signature events''; such events occurred even after the cessation of stimuli (29). This is likely to be species specific since we failed to see the ''signature events'' in the analogous V17C mutant from Eco-MscL. But notably, in the previous study the authors found that the Tb-MscL crystal structure does not predict that the V15 residues can easily interact with one another within the channel complex, and therefore proposed that their findings were likely to be the result of asymmetric movements that often occur upon gating. A similar argument can be made for the trapping of the Eco-MscL N15 mutant. As discussed above and presented in Table 2, N15 seems unlikely to interact in any known or predicted conformation if a smooth, radially symmetric closed-to-open transition is assumed, yet the disulfide bridging observed is very efficient. In the case of the V15C Tb-MscL, once the disulfide bridge is formed, the channel appears to lock into an unstable open structure and presumably attains unnatural and irreversible conformational states under the strain. Here we have apparently trapped N15C Eco-MscL in a normal transition state that does not irreversibly misfold, but instead retains the capacity to obtain both fully closed and fully open channel states.

The authors thank Dr. Paul Moe for critical helpful discussions and critical reading of the manuscript.

This work was supported by grant I-1420 of the Welch Foundation, grant FA9550-05-1-0073 of the Air Force Office of Scientific Review, grant 0655012Y of the American Heart Association-Texas Affiliate, and grant GM61028 from the National Institutes of Health.

REFERENCES

1. Niu, W., and F. Sachs. 2003. Dynamic properties of stretch-activated K^+ channels in adult rat atrial myocytes. *Prog. Biophys. Mol. Biol.* 82:121–135.
2. Tan, J., W. Liu, and D. Saint. 2004. Differential expression of the mechanosensitive potassium channel TREK-1 in epicardial and endocardial myocytes in rat ventricle. *Exp. Physiol.* 89:237–242.
3. Terrenoire, C., I. Lauritzen, F. Lesage, G. Romey, and M. Lazdunski. 2001. A TREK-1-like potassium channel in atrial cells inhibited by b-adrenergic stimulation and activated by volatile anesthetics. *Circ. Res.* 89:336–342.
4. Hamill, O. P., and B. Martinac. 2001. Molecular basis of mechanotransduction in living cells. *Physiol. Rev.* 81:685–740.
5. Sukharev, S., and D. P. Corey. 2004. Mechanosensitive channels: multiplicity of families and gating paradigms. *Sci. STKE.* 2004:re4.
6. Berrier, C., M. Besnard, B. Ajouz, A. Coulombe, and A. Ghazi. 1996. Multiple mechanosensitive ion channels from *Escherichia coli*, activated at different thresholds of applied pressure. *J. Membr. Biol.* 151: 175–187.
7. Li, Y., P. C. Moe, S. Chandrasekaran, I. R. Booth, and P. Blount. 2002. Ionic regulation of MscK, a mechanosensitive channel from *Escherichia coli*. *EMBO J.* 21:5323–5330.
8. McLaggan, D., M. A. Jones, G. Gouesbet, N. Levina, S. Lindey, W. Epstein, and I. R. Booth. 2002. Analysis of the kefA2 mutation suggests that KefA is a cation-specific channel involved in osmotic adaptation in *Escherichia coli*. *Mol. Microbiol.* 43:521–536.
9. Levina, N., S. Totemeyer, N. R. Stokes, P. Louis, M. A. Jones, and I. R. Booth. 1999. Protection of *Escherichia coli* cells against extreme turgor by activation of MscS and MscL mechanosensitive channels: identification of genes required for MscS activity. *EMBO J.* 18:1730–1737.
10. Sukharev, S. I., P. Blount, B. Martinac, F. R. Blattner, and C. Kung. 1994. A large-conductance mechanosensitive channel in *E. coli* encoded by *mscL* alone. *Nature.* 368:265–268.
11. Blount, P., S. I. Sukharev, P. C. Moe, M. J. Schroeder, H. R. Guy, and C. Kung. 1996. Membrane topology and multimeric structure of a mechanosensitive channel protein of *Escherichia coli*. *EMBO J.* 15:4798–4805.
12. Blount, P., and P. Moe. 1999. Bacterial mechanosensitive channels: integrating physiology, structure and function. *Trends Microbiol.* 7:420–424.
13. Yoshimura, K., A. Batiza, M. Schroeder, P. Blount, and C. Kung. 1999. Hydrophilicity of a single residue within MscL correlates with increased channel mechanosensitivity. *Biophys. J.* 77:1960–1972.
14. Chang, G., R. H. Spencer, A. T. Lee, M. T. Barclay, and D. C. Rees. 1998. Structure of the MscL homolog from *Mycobacterium tuberculosis*: a gated mechanosensitive ion channel. *Science.* 282:2220–2226.
15. Sukharev, S., M. Betanzos, C. Chiang, and H. Guy. 2001. The gating mechanism of the large mechanosensitive channel MscL. *Nature.* 409: 720–724.
16. Sukharev, S., S. Durell, and H. Guy. 2001. Structural models of the MscL gating mechanism. *Biophys. J.* 81:917–936.
17. Perozo, E., D. M. Cortes, P. Sompornpisut, A. Kloda, and B. Martinac. 2002. Open channel structure of MscL and the gating mechanism of mechanosensitive channels. *Nature.* 418:942–948.
18. Bartlett, J. L., G. Levin, and P. Blount. 2004. An *in vivo* assay identifies changes in residue accessibility on mechanosensitive channel gating. *Proc. Natl. Acad. Sci. USA.* 101:10161–10165.
19. Blount, P., S. I. Sukharev, M. J. Schroeder, S. K. Nagle, and C. Kung. 1996. Single residue substitutions that change the gating properties of a mechanosensitive channel in *Escherichia coli*. *Proc. Natl. Acad. Sci. USA.* 93:11652–11657.
20. Ou, X., P. Blount, R. J. Hoffman, and C. Kung. 1998. One face of a transmembrane helix is crucial in mechanosensitive channel gating. *Proc. Natl. Acad. Sci. USA.* 95:11471–11475.
21. Kumánovics, A., G. Levin, and P. Blount. 2002. Family ties of gated pores: evolution of the sensor module. *FASEB J.* 16:1623–1629.
22. Levin, G., and P. Blount. 2004. Cysteine scanning of MscL transmembrane domains reveals residues critical for mechanosensitive channel gating. *Biophys. J.* 86:2862–2870.
23. Moe, P. C., G. Levin, and P. Blount. 2000. Correlating a protein structure with function of a bacterial mechanosensitive channel. *J. Biol. Chem.* 275:31121–31127.

24. Norman, C., Z. W. Liu, P. Rigby, A. Raso, Y. Petrov, and B. Martinac. 2005. Visualisation of the mechanosensitive channel of large conductance in bacteria using confocal microscopy. *Eur. Biophys. J.* 34:396–402.

25. Blount, P., S. I. Sukharev, P. C. Moe, B. Martinac, and C. Kung. 1999. Mechanosensitive channels of bacteria. *In* Methods in Enzymology. P. M. Conn, editor. Academic Press, San Diego, CA. 458–482.

26. Maurer, J. A., and D. A. Dougherty. 2003. Generation and evaluation of a large mutational library from the *Escherichia coli* mechanosensitive channel of large conductance, MscL: implications for channel gating and evolutionary design. *J. Biol. Chem.* 278:21076–21082.

27. Ajouz, B., C. Berrier, A. Garrigues, M. Besnard, and A. Ghazi. 1998. Release of thioredoxin via the mechanosensitive channel MscL during osmotic downshock of *Escherichia coli* cells. *J. Biol. Chem.* 273: 26670–26674.

28. Batiza, A. F., M. M. Kuo, K. Yoshimura, and C. Kung. 2002. Gating the bacterial mechanosensitive channel MscL *in vivo*. *Proc. Natl. Acad. Sci. USA.* 99:5643–5648.

29. Shapovalov, G., R. Bass, D. C. Rees, and H. A. Lester. 2003. Open-state disulfide crosslinking between mycobacterium tuberculosis mechanosensitive channel subunits. *Biophys. J.* 84:2357–2365.

30. Falke, J. J., A. F. Dernburg, D. A. Sternberg, N. Zalkin, D. L. Milligan, and D. E. Koshland Jr. 1988. Structure of a bacterial sensory receptor. A site-directed sulfhydryl study. *J. Biol. Chem.* 263:14850–14858.

31. Srinivasan, N., R. Sowdhamini, C. Ramakrishnan, and P. Balaram. 1990. Conformations of disulfide bridges in proteins. *Int. J. Pept. Protein Res.* 36:147–155.

32. Perozo, E., A. Kloda, D. M. Cortes, and B. Martinac. 2001. Site-directed spin-labeling analysis of reconstituted Mscl in the closed state. *J. Gen. Physiol.* 118:193–206.

33. Iscla, I., G. Levin, R. Wray, R. Reynolds, and P. Blount. 2004. Defining the physical gate of a mechanosensitive channel, MscL, by engineering metal-binding sites. *Biophys. J.* 87:3172–3180.

34. Holmgren, M., K. S. Shin, and G. Yellen. 1998. The activation gate of a voltage-gated K+ channel can be trapped in the open state by an intersubunit metal bridge. *Neuron.* 21:617–621.

35. Liu, Y., M. Holmgren, M. E. Jurman, and G. Yellen. 1997. Gated access to the pore of a voltage-dependent K^+ channel. *Neuron.* 19:175–184.

36. Rothberg, B. S., K. S. Shin, P. S. Phale, and G. Yellen. 2002. Voltage-controlled gating at the intracellular entrance to a hyperpolarization-activated cation channel. *J. Gen. Physiol.* 119:83–91.

37. Rothberg, B. S., K. S. Shin, and G. Yellen. 2003. Movements near the gate of a hyperpolarization-activated cation channel. *J. Gen. Physiol.* 122: 501–510.

38. Webster, S. M., D. del Camino, J. P. Dekker, and G. Yellen. 2004. Intracellular gate opening in Shaker K+ channels defined by high-affinity metal bridges. *Nature.* 428:864–868.